

# Photoassociation spectroscopy of a Spin-1 Bose-Einstein condensate

C.D. Hamley, E.M. Bookjans, G. Behin-Aein, P. Ahmadi, and M.S. Chapman  
*School of Physics, Georgia Institute of Technology, Atlanta, GA 30332-0430*

We report on the high resolution photoassociation spectroscopy of a  $^{87}\text{Rb}$  spin-1 Bose-Einstein condensate to the  $1_g(P_{3/2}) v = 152$  excited molecular states. We demonstrate the use of spin dependent photoassociation to experimentally identify the molecular states and their corresponding initial scattering channel. These identifications are in excellent agreement with the eigenvalues of a hyperfine-rotational Hamiltonian. Using the observed spectra we estimate the change in scattering length and identify photoassociation laser light frequency ranges that maximize the change in the spin-dependent mean-field interaction energy.

PACS numbers: 34.50.Rk, 33.15.Pw

In a spinor Bose-Einstein condensate [1, 2, 3, 4], the delicate interplay between different atomic spin orientations results in a small spin dependence of the collisional interaction energy [5]. Though the spin dependence is small relative to the total interaction energy (*e.g.*  $\sim 0.5\%$  in  $^{87}\text{Rb}$ ), the coherence of the condensate allows observation of novel phenomena such as coherent spin mixing and dynamics [6, 7, 8, 9, 10], metastable states [11], spin domains [12, 13] and quantum tunneling across spin domains [14]. The spin-dependent interaction energy arises from the small difference in the *s*-wave scattering lengths of the allowed angular momentum channels and manifests in anti- or ferromagnetic properties for a spin-1 condensate depending on the algebraic sign of the difference. In the two spin-1 condensates investigated to date,  $^{23}\text{Na}$  and  $^{87}\text{Rb}$ , the former is anti-ferromagnetic and the latter is ferromagnetic.

Magnetic [15] and optical [16] Feshbach resonances have been employed to dynamically change the scattering lengths which offers the tantalizing prospect of influencing the spinor dynamics or even possibly changing the magnetic nature of the condensate. However, spinor dynamics are suppressed for magnetic fields greater than a few 100s of mG [7, 17]. The fields used in magnetic Feshbach resonance experiments are much larger than this and thus can not be used for altering the spinor dynamics. Photoassociation around single resonance lines also has limited flexibility since the atom loss rate is very high near the resonances where the change in scattering lengths is appreciable. To circumvent this problem it has been suggested to use the effect of multiple photoassociation lines from a vibrational level with a rich hyperfine structure [18]. This allows parameters that depend on multiple scattering lengths to be enhanced between lines from different scattering channels while the atom loss rate is reduced. Specifically, variation of the spin dependent interaction strength could be optimized if there are adjacent molecular states that occur through different scattering channels. In order to identify the existence of such lines, collision channel selective spectroscopy needs to be performed which requires control over the Zeeman states of the colliding atoms. Note that although the

effects of hyperfine levels of the colliding atoms on the photoassociation spectrum has been previously observed [19, 20], there has not been any collision channel selective spectroscopy.

In this Letter, we report on experimental photoassociation spectroscopy of a spinor condensate. By observing the effect of the Zeeman states of the colliding atoms on the photoassociation spectrum, we extract information about the angular momentum of the molecular states. We identify for the first time molecular states that are allowed for a specific scattering channel while forbidden for another. From the spectrum, we calculate the atom loss rate and the expected change in the mean-field interaction energy. Using the observed spectra and these calculations, we identify suitable photoassociation light frequencies that maximize change of the spin dependent interaction strength with modest atom loss rates.

The experiment is performed on  $^{87}\text{Rb}$  condensates created directly in an optical trap [1]. After the condensate is formed, it is exposed to a photoassociation (PA) laser. To measure the spectrum of the molecular excited states, the condensate population losses are measured for different frequencies of the PA light. The PA excitation laser frequency is tuned near the  $1_g(P_{3/2}) v = 152$  state which has a rich hyperfine structure and a binding energy of  $24.1 \text{ cm}^{-1}$  [21, 22] below the  $D_2$  line of  $^{87}\text{Rb}$ . The PA laser has a focused waist of  $80 \mu\text{m}$ , and its frequency is actively stabilized with an accuracy  $\sim 5 \text{ MHz}$  using a transfer cavity locked to a stabilized diode laser. Fig. 1 shows the observed photoassociation spectrum of the  $1_g(P_{3/2}) v = 152$  state taken using condensates with  $|f = 1, m_f = -1\rangle$  and  $|f = 1, m_f = 0\rangle$  spin states. A portion of the  $|f = 1, m_f = -1\rangle$  spectrum was observed in [22]. The PA light is ramped up to  $3.8 \text{ mW}$  in  $50 \text{ ms}$ , after which it remains on for  $100 \text{ ms}$ . Successive data points are separated by  $5 \text{ MHz}$ . The weaker lines identified by  $\kappa$  through  $\pi$  have been confirmed using more intensity and longer time but are shown here under the same conditions as the stronger lines for consistency. The inset shows a line too weak to be made out in the larger scan. In order to enhance the visibility of this line, the PA light power is increased to  $11 \text{ mW}$  and left on for

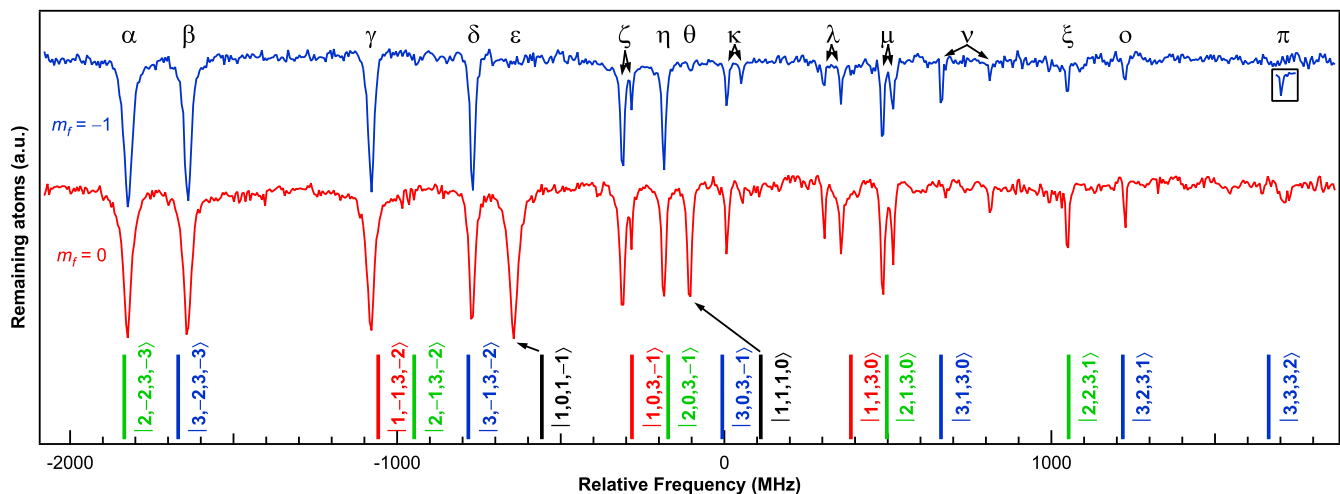


FIG. 1: Observed photoassociation spectrum of the  $1_g(P_{3/2}) v = 152$  state for  $m_f = -1$  (upper) and  $m_f = 0$  (lower). These spectra are obtained after 150 ms of exposing a BEC to a PA light with 3.8 mW and 80 micron beam waist. The inset box for  $m_f = -1$  is obtained using 350 ms and 11 mW with averaging to enhance visibility of this weaker line. Plots are offset for clarity. The origin of the hyperfine-rotation Hamiltonian fit is used as the zero point for the plot. A stick spectrum with approximate  $|F, f, I, i\rangle$  labels is given.

300 ms, and it has been averaged over four scans. For each data point, an absorptive image of the condensate is taken 12 ms after the PA and trapping lasers are turned off. The condensate population is counted and normalized to an average value taken under the same conditions but with the PA light frequency detuned far from any of the molecular lines observed in Fig. 1.

The  $1_g$  potential is categorized as a Hund's case (c). The relevant good quantum numbers for this potential are total molecular angular momentum,  $F$ , total nuclear spin,  $I$ , and  $\Omega$ , the projection of the rotational angular momentum,  $J$ , on the internuclear axis. For this case, the projections  $F_z$ ,  $I_z$  of  $\vec{F}$  and  $\vec{I}$  on the internuclear axis are almost good quantum numbers, while  $J$  is not [23].

The possible values of  $F$  are determined by bosonic symmetry and angular momentum addition rules. For two identical spin-1 bosons, the allowed  $s$ -wave collision channels are  $F = 2$  or  $0$ . Addition of the angular momentum of the colliding atoms and the PA photon specifies the possible total angular momentum,  $F$ , of the available molecular states for each scattering channel. Photoassociation through the total spin 2 scattering channel gives molecular  $F$  numbers of 1, 2, and 3 while the total spin 0 scattering channel restricts  $F$  to 1.

In the following, we use the experimental properties of the photoassociation spectrum to identify these quantum numbers for the observed molecular lines. The most striking difference between the two PA spectra in Fig. 1 is that the lines  $\varepsilon$  and  $\theta$  appear only for the condensate containing the  $m_f = 0$  spin state. Since two  $m_f = -1$  atoms can only scatter through the total spin 2 channel, while two  $m_f = 0$  atoms access both the total spin 2 and

0 channels, this observation indicates that these lines occur through the total spin 0 scattering channel, restricting  $F$  for the molecular state represented by these lines to 1. This conclusion is further confirmed by repeating the same experiment with condensates containing both  $m_f = -1$  and  $m_f = 1$  spin states and also with condensates containing  $m_f = -1$  and  $m_f = 0$  (see Fig. 2). These spin state combinations are prepared using a microwave manipulation technique similar to the one used in Ref. [7]. The populations of different  $m_f$  states are counted by spatially separating them using a Stern-Gerlach field during the time of flight. An  $m_f = -1$  ( $m_f = 1$ ) can only access the total spin 0 scattering channel through collision with an  $m_f = 1$  ( $m_f = -1$ ) spin state. Therefore, neither of these spin states participate in the total spin 0 channel photoassociation if they coexist in the condensate only with an  $m_f = 0$  spin state. To illustrate these predictions, PA spectra across the lines  $\varepsilon$  and  $\theta$  are taken with condensates containing different mixtures of spin states as shown in Fig. 2.

The data shown in Figs. 2(a) and 2(b) are taken with similar conditions to Fig. 1, whereas in Fig. 2(c) and 2(d) the photoassociation power is decreased to 1.5 mW to reduce the mechanical effects on the  $m_f = -1$  atoms caused by the rapid loss of the  $m_f = 0$  atoms from the trap. These spectra are taken with frequency steps of 2 MHz. The observed data in this figure shows that the  $m_f = -1$  and  $m_f = 1$  spin states participate in the photoassociation for the lines  $\varepsilon$  and  $\theta$  if both of them coexist in the condensate, whereas if  $m_f = -1$  spin state coexists with the  $m_f = 0$  spin state it does not participate in the photoassociation process. This observation matches

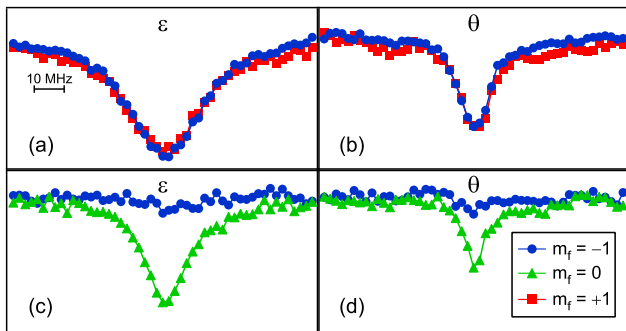


FIG. 2: Photoassociation spectroscopy of  $\varepsilon$  and  $\theta$  with different mixtures of spin states. (a) and (b) Lines  $\varepsilon$  and  $\theta$  for mixture of  $m_f = -1$  and  $m_f = 1$  spin states. (c) and (d) for mixture of  $m_f = -1$  and  $m_f = 0$ . The observed data points corresponding to  $m_f = (-1, 0, 1)$  spin states are represented by circles, triangles, and squares respectively.

our analysis based on scattering channels and confirms that  $F = 1$  for lines  $\varepsilon$  and  $\theta$ .

To identify  $F = 2$  PA lines we note that a  $\Delta F = 0$ ,  $\Delta M_F = 0$  transition from a total two atom collisional spin state  $|2, 0\rangle$  to a bound molecular state  $|2, 0\rangle$  is forbidden by the electric dipole selection rule. Therefore the lines with  $F = 2$  are suppressed for an  $m_f = 0$  spin state condensate with  $\pi$ -polarized PA light. Such lines are found by taking a PA spectrum of a pure  $m_f = 0$  condensate in the presence of an external B-field of 1 G along the polarization of the PA light. The observed data for this case, shown in Fig. 3, indicates that the lines  $\alpha$ ,  $\eta$ ,  $\mu$ , and  $\xi$  are absent. By changing the polarization of the PA light perpendicular to the quantization axis defined by the applied B-field, all of these lines reappear in the spectrum. A comparison between the observed data with polarization aligned parallel (square) and perpendicular (circle) to the external B-field is shown in Fig. 3, which confirms  $F = 2$  as a good quantum number for these lines. Fig. 3(c) also indicates that the line  $\mu$  is split into two  $F = 2$  components.

From these observations and the spacing of the lines we are able to assign  $F$  and  $I$  for the observed lines. This is accomplished by noting that for possible values of  $F = 1, 2$ , and  $3$  the eigenvalues of  $\vec{F}^2$  are 2, 6, and 12. Therefore the separation between molecular states with  $F = 1$  and  $2$  should be  $2/3$  of the frequency separation between the lines with  $F = 2$  and  $3$ .  $F$  numbers for the remaining lines are readily deduced by their spacing and order in each hyperfine grouping. The total nuclear spin for these lines is found by decomposing the initial scattering wave function of the two colliding atoms. This analysis shows that the total nuclear spin must be 1 for the total spin 0 scattering channel and predominantly  $I = 3$  for the total spin 2 scattering channel. Table I gives the assigned values of  $F$  and  $I$  for the observed lines.

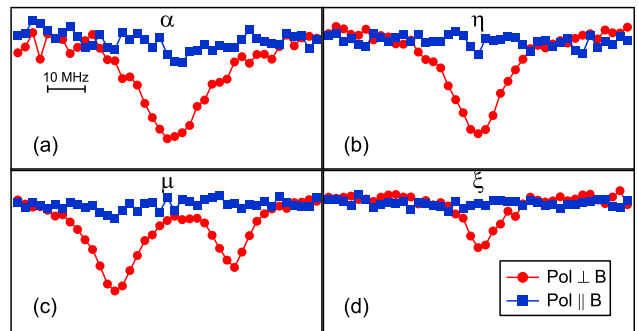


FIG. 3: Photoassociation spectroscopy through lines  $\alpha$ ,  $\eta$ ,  $\mu$ , and  $\xi$  for an  $m_f = 0$  spin state condensate to an  $F = 2$  molecular state. The data points are taken with the polarization vector of the PA light along and perpendicular to an external magnetic field (squares) and (circles).

TABLE I: Assigned total angular momentum and nuclear spin of the molecular states appearing in the PA spectra of Fig. 1.

	$\alpha$	$\beta$	$\gamma$	$\delta$	$\varepsilon$	$\zeta$	$\eta$	$\theta$	$\kappa$	$\lambda$	$\mu$	$\nu$	$\xi$	$o$	$\pi$
$F$	2	3	1	3	1	1	2	1	3	1	2	3	2	3	3
$I$	3	3	3	3	1	3	3	1	3	3	3	3	3	3	3

For the  $1_g$  potential, the molecular hyperfine constant is comparable to the small rotational constant of the state. Therefore, the effective Hamiltonian for the  $1_g$  rotation-hyperfine structure can be written as [23],

$$\begin{aligned}
 H_{H-R} &= a_v \vec{I} \cdot \vec{\Omega} + B_v \vec{J}^2 \\
 &= a_v I_{\bar{z}} \Omega \\
 &\quad + B_v \{ \vec{F}^2 + \vec{I}^2 - 2F_{\bar{z}} I_{\bar{z}} - \bar{F}_+ \bar{I}_- - \bar{F}_- \bar{I}_+ \}, \quad (1)
 \end{aligned}$$

where the operators are defined with respect to the internuclear axis  $\bar{z}$ . Since changing the signs of  $F_{\bar{z}}$ ,  $I_{\bar{z}}$ , and  $\Omega$  results in a degenerate state, the states are labeled by  $F$ ,  $f$ ,  $I$ , and  $i$ , where  $f = F_{\bar{z}} \cdot \Omega$  and  $i = I_{\bar{z}} \cdot \Omega$ . The eigenvalues of the Hamiltonian are obtained by diagonalizing its corresponding matrix in the  $|F, F_{\bar{z}}, I, I_{\bar{z}}\rangle$  basis set. The coupling is sufficiently weak that labeling the final states by the almost good quantum numbers of  $f$  and  $i$  is justified. These eigenvalues are fit to the observed spectrum of the  $m_f = -1$  condensate of Fig. 1 using the least squares approach with  $a_v$ ,  $B_v$ , and the frequency offset  $\omega_{\text{offset}}$  as fitting parameters. In case of the split lines, the stronger one is used for fitting. Using the  $a_{F=2}$  lines the fitting specifies  $a_v$  and  $B_v$  to be 667(5) and 27.6(1.3) MHz, respectively. The positions of the eigenvalues using these parameters are shown as a stick spectrum in Fig. 1 which is in good agreement with the observed locations of the atom loss lines in the PA spectrum. The stick spectrum is labeled by the dominant part of the corresponding eigenvectors which is in complete agreement with the assigned quantum numbers

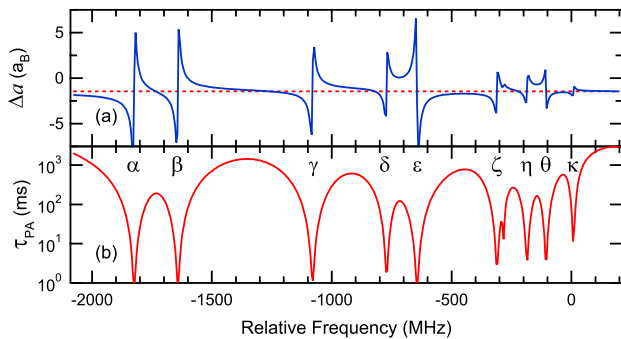


FIG. 4: Calculated values for  $\Delta a$  and for the PA limited lifetime of BEC. The dotted line is the nominal value of  $\Delta a$ . The intensity here is 20 times that used to take the spectra in Fig. 1.

in Table I.

A few general comments should be made for the observed as well as predicted spectra. First, the molecular state corresponding to the  $|2, -1, 3, -2\rangle$  eigenstate is not observed under any experimental condition. This line is also absent in a scan of the  $v = 153$  vibrational level. Second, predicted locations of the lines  $\varepsilon$  and  $\theta$  corresponding to the  $a_{F=0}$  scattering channel are in poorer agreement with their observed locations compared to the other lines. These two lines are connected by arrows to their assumed eigenvalues in Fig. 1. There appears to be a discrepancy both in the separation of the lines and their apparent origin for the hyperfine-rotation Hamiltonian. It was unclear as to whether different fit parameters or a revision to the Hamiltonian is needed to correct the deviations. Last, we note that some of the lines appear to be split on the order of 30 to 160 MHz. These split lines are connected to their labels in Fig. 1 for clarity. The Hamiltonian presented in Eq. (1) predicts that all lines should be doubly degenerate and does not account for this splitting. This points to an additional interaction not considered in this simple model. These discrepancies are important for refinement of the molecular potential theory.

One of our motivations for studying this system is to assess the suitability of photoassociation induced change in two  $s$ -wave scattering lengths,  $\Delta a = a_{F=2} - a_{F=0}$ , in order to manipulate spin-dependent properties of a condensate. To determine the variation of  $\Delta a$ , the observed data of Fig. 1 is fitted to a theoretical formula for the inelastic loss rate ( $K_{\text{inel}}$ ) to find the width and amplitude for each line as discussed in Ref. [16]. These fit parameters along with the condensate density ( $n_0$ ) are then used to calculate the estimated change in  $\Delta a$  as shown in Fig. 4(a).

We also calculate a photoassociation limited lifetime,  $\tau_{PA} = (K_{\text{inel}} \times n_0)^{-1}$ , during which spin dependent dynamics can be observed before the condensate is depleted

by the PA atom loss as shown in Fig. 4(b). The plots in Fig. 4 assume a PA intensity 20 times higher than that used to measure the spectrum. One of the more interesting frequency ranges in Fig. 4 is between lines  $\delta$  and  $\varepsilon$  which are associated with different scattering channels. In this frequency range the influences of the two lines reinforce each other for a large change in  $\Delta a$ , but with only a modest reduction in the 3 s lifetime of the condensate due to the PA light. From this data it is clear that the value of  $\Delta a$  can be altered significantly from its nominal value of  $1.45(32)a_B$  [7] up to a total cancellation, with sufficient PA limited lifetimes needed to see the change in spinor dynamics. However to change the sign and hence the magnetic nature of the condensate, the values needed correspond to challengingly short lifetimes compared to the time needed to relax to the magnetic ground state. Hopefully, other molecular states will have a slightly more favorable width, amplitude, or spacing.

In conclusion, we performed photoassociation spectroscopy on a spin-1 condensate. The spin dependent photoassociation spectrum is used to identify good quantum numbers for some of the molecular states, which are in agreement with theoretical predictions of a hyperfine-rotation Hamiltonian. The spectrum is also used to predict the photoassociation limited lifetime and change in  $\Delta a$ . It is shown that optical Feshbach resonances to a molecular state with hyperfine structure are a viable method of altering the spin-dependent mean-field interaction energy to change the spinor dynamics of the condensate. The results of this study provide a valuable test case to answer general questions about how to model molecular potentials in the presence of hyperfine and rotation interactions. A high resolution photoassociation study of other vibrational levels will provide a deeper understanding of molecular potentials. This work is supported by the National Science Foundation, PHYS-0605049.

- 
- [1] M.D. Barrett *et al.*, Phys. Rev. Lett. **87**, 010404 (2001).
  - [2] E.A. Cornell *et al.*, J. Low Temp. Phys. **113**, 151 (1998).
  - [3] C.J. Myatt *et al.*, Phys. Rev. Lett. **78**, 586 (1997).
  - [4] D.M. Stamper-Kurn *et al.*, Phys. Rev. Lett. **80**, 2027 (1998).
  - [5] T.L. Ho, Phys. Rev. Lett. **81**, 742 (1998).
  - [6] M.S. Chang *et al.*, Phys. Rev. Lett. **92**, 140403 (2004).
  - [7] M.S. Chang *et al.*, Nat. Phys. **1**, 111 (2005).
  - [8] W.X. Zhang *et al.*, Phys. Rev. A **72**, 013602 (2005).
  - [9] H. Schmaljohann *et al.*, Phys. Rev. Lett. **92**, 040402 (2004).
  - [10] A. Widera *et al.*, Phys. Rev. Lett. **95**, 190405 (2005).
  - [11] H.J. Miesner *et al.*, Phys. Rev. Lett. **82**, 2228 (1999).
  - [12] J. Stenger *et al.*, Nature **396**, 345 (1998).
  - [13] L.E. Sadler *et al.*, Nature **443**, 312 (2006).
  - [14] D.M. Stamper-Kurn *et al.*, Phys. Rev. Lett. **83**, 661 (1999).

- [15] S. Inouye *et al.*, Nature **392**, 151 (1998).
- [16] M. Theis *et al.*, Phys. Rev. Lett. **93**, 123001 (2004).
- [17] M. Erhard, Appl. Phys. B **79**, 1001 (2004).
- [18] M.W. Jack, and M. Yamashita, Phys. Rev. A **71**, 033619 (2005).
- [19] E.R.I. Abraham *et al.*, Phys. Rev. A **53**, 3092 (1996).
- [20] E. Tiesinga *et al.*, Phys. Rev. A **71**, 052703 (2005).
- [21] J.D. Miller *et al.*, Phys. Rev. Lett. **71**, 2204 (1993).
- [22] M. Theis, "Optical Feshbach Resonances in a Bose-Einstein Condensate," doctoral thesis (University of Innsbruck, 2005).
- [23] X.T. Wang *et al.*, Phys. Rev. A **57**, 4600 (1998).